VNUHCM Journal of Health Sciences 2026, 7(2):1156-1172

Open Access Full Text Article

Research Article

Phytochemical study, antioxidant activity, and molecular docking analysis of sterols from *Calotropis gigantea* leaves

Le Viet Ha Tran*, Thanh Duy Huynh, Thi Hong Hieu Nguyen, Thi My Duyen Chung

ABSTRACT

Introduction: *Calotropis gigantea* (L.) R. Br. ex Schult. has long been used in traditional medicine for the management of inflammatory disorders and conditions associated with oxidative stress. Previous studies have reported that this species contains diverse secondary metabolites with promising biological activities; however, the phytochemical profile of leaf extracts prepared with different solvent polarities and the potential antioxidant mechanisms of their major constituents remain insufficiently characterized.

Objective: This study aimed to investigate the phytochemical composition, antioxidant and antibacterial activities of aqueous and ethanolic leaf extracts of *C. gigantea*, isolate major bioactive constituents from the most active extract, and explore their potential antioxidant-related mechanisms through molecular docking analysis.

Methods: Leaves of *C. gigantea* were extracted using water and ethanol (40%, 70%, and 96%). Preliminary phytochemical screening was performed using standard qualitative assays. Antioxidant activity was evaluated by DPPH and ABTS radical scavenging assays, while antibacterial activity was assessed against seven bacterial strains using the agar well diffusion method. The extract showing the highest antioxidant activity was subjected to chromatographic fractionation, and isolated compounds were identified by ^{1}H-NMR spectroscopy. Molecular docking was conducted to evaluate the interactions of the isolated compounds with antioxidant-related targets, including superoxide dismutase 1 (SOD1), catalase (CAT), and Kelch-like ECH-associated protein 1 (Keap1).

Results: Phytochemical screening revealed the presence of alkaloids, phenolic compounds, flavonoids, coumarins, sterols, terpenoids, reducing sugars, and saponins, with ethanolic extracts containing higher levels of phenolic and terpenoid constituents than the aqueous extract. Among the tested samples, the 70% ethanol extract exhibited the strongest antioxidant activity, reaching 86.31 ± 1.10% DPPH radical scavenging at 1000 μg/mL and 44.54 ± 0.87% ABTS radical scavenging at 100 μg/mL. No antibacterial activity was observed for any extract under the experimental conditions. Phytochemical investigation of the most active extract resulted in the isolation of β-sitosterol (**1**) and β-sitostenone (**2**). Molecular docking demonstrated favorable binding of both sterols to SOD1, CAT, and especially Keap1, with β-sitostenone exhibiting the strongest predicted binding affinity (−10.3 kcal/mol) toward Keap1.

Conclusions: The findings suggest that 70% ethanol is the most suitable solvent for extracting antioxidant-associated phytochemicals from *C. gigantea* leaves. The isolation of β-sitosterol and β-sitostenone, together with their favorable interactions with antioxidant-related targets, particularly Keap1, suggests that these sterols may contribute to the antioxidant activity of *C. gigantea* through modulation of the Keap1/Nrf2 signaling pathway. These results provide a scientific basis for further mechanistic and in vivo studies to support the development of *C. gigantea*-derived antioxidant agents.

Keywords: *Calotropis gigantea*, sterol, antioxidant activity, molecular docking

Faculty of Traditional Medicine, University of Medicine and Pharmacy at Ho Chi Minh City, Vietnam

Correspondence

Le Viet Ha Tran, Faculty of Traditional Medicine, University of Medicine and Pharmacy at Ho Chi Minh City, Vietnam

Email: tlvha@ump.edu.vn

History

- Received: 15-05-2026
- Revised: 04-07-2026
- Accepted: 20-07-2026
- Published Online: 14-09-2026

DOI : https://doi.org/10.32508/vnuhcmjhs.v7i2.788

Check for updates

INTRODUCTION

Oxidative stress resulting from excessive reactive oxygen species (ROS) generation is strongly linked to inflammation, metabolic disorders, neurodegenerative diseases, and other chronic pathological conditions. Endogenous antioxidant defense mechanisms, such as superoxide dismutase 1 (SOD1), catalase (CAT), and the Kelch-like ECH-associated protein 1 (Keap1) signaling pathway, contribute substantially to cellular redox homeostasis and protection against oxidative injury [1,2].

Calotropis gigantea (L.) R. Br. ex Schult. is a medicinal plant traditionally used for the treatment of inflammation, skin diseases, respiratory disorders, and other ailments. Previous studies have reported that this plant contains diverse secondary metabolites, such as flavonoids, alkaloids, phenolics, terpenoids, steroids/triterpenoids, tannins, and saponins, which

Cite this article : Tran L V H, Huynh T D, Nguyen T H H, Chung T M D. **Phytochemical study, antioxidant activity, and molecular docking analysis of sterols from *Calotropis gigantea* leaves**. *VNUHCM J. Health Sci.* 2026; 7(2):1156-1172.

may contribute to its antioxidant and other pharmacological activities[3]. However, the phytochemical characteristics and antioxidant potential of *C. gigantea* leaves extracted with solvents of different polarities remain insufficiently explored.

Solvent polarity strongly influences the extraction efficiency of bioactive compounds and, consequently, the biological activity of plant extracts. Therefore, comparing aqueous and ethanolic extracts may help clarify the relationship between phytochemical composition and antioxidant capacity. In addition to direct radical scavenging assays, molecular docking with antioxidant-related targets such as SOD1, CAT, and Keap1 can provide preliminary insight into possible mechanisms of action.

In this study, *C. gigantea* leaf extracts prepared using water and different concentrations of ethanol were investigated for their phytochemical composition, antioxidant activity using DPPH and ABTS assays, and antibacterial activity. Furthermore, the interactions of the isolated compounds β-sitosterol and β-sitostenone with SOD1, CAT, and Keap1 were evaluated by molecular docking to suggest their potential role in oxidative stress modulation. To the best of our knowledge, no previous study has comprehensively investigated the antioxidant activity of *C. gigantea* leaf extracts prepared using different ethanol concentrations together with molecular docking analysis of isolated sterols toward antioxidant-related targets, including Keap1, SOD1, and CAT.

MATERIALS AND METHODS

Plant material

Leaves of *Calotropis gigantea* (L.) R. Br. ex Schult. were collected from mature plants in Ho Chi Minh City, Vietnam, in September 2024. The plant material was taxonomically authenticated by specialists at the Institute of Medicinal Materials, Vietnam. A voucher specimen (Voucher No. MNP0019_01) was deposited at the Department of Traditional Medicine, University of Medicine and Pharmacy at Ho Chi Minh City, Vietnam, for future reference. The morphological characteristics of the authenticated plant specimen are provided in Figure 5.

Extraction procedure

Powdered leaves of *C. gigantea* (500 g) were extracted using distilled water and ethanol at concentrations of 40%, 70%, and 96%. The aqueous extract was prepared by decoction with distilled water (1:15, w/v) in three successive cycles (30 min, followed by two 15 min extractions). For ethanolic extracts, the powdered material was separately macerated with each ethanol concentration at room temperature and extracted three times. After collection, the filtrates were combined and concentrated under reduced pressure to produce crude extracts, followed by storage at 4 °C until subsequent analysis.

Phytochemical screening

Preliminary phytochemical evaluation of *C. gigantea* leaf extracts was performed using standard qualitative assays to determine the presence of major groups of secondary metabolites. The extracts were screened for alkaloids, saponins, reducing sugars, phenolic compounds, flavonoids, coumarins, and steroids/triterpenoids. Alkaloids were detected using Mayer's reagents, while saponins were identified based on frothing tests. Reducing sugars were determined using Fehling's test. Phenolic compounds and tannins were detected using ferric chloride ($FeCl_3$), whereas flavonoids were identified using lead acetate reagent according to the method described by Kori[4]. Coumarins were tested using sodium hydroxide solution, and terpenoids were detected using the Salkowski reaction as described by Harborne[5]. The presence or absence of each phytochemical group was recorded based on characteristic color changes or precipitate formation. The intensity of reactions was qualitatively expressed as weak (+), moderate (++), or strong (+++), depending on the observed response.

Antioxidant activity

DPPH radical scavenging assay

The DPPH radical scavenging capacity of the extracts was determined using a 96-well microplate format. Briefly, the DPPH reagent was prepared in methanol, whereas extract samples were dissolved in ethanol and prepared at concentrations of 1, 10, 100, and 1000 μg/mL. The reaction mixture, consisting of 150 μL of ethanol, 25 μL of DPPH solution, and 25 μL of extract solution, was incubated at room temperature in the dark for 30 min. Absorbance was then recorded at 515 nm using a microplate reader. Radical scavenging activity was calculated using the following formula: Scavenging activity (%) = $[(A_0 - A_1) / A_0] \times 100$, where A_0 is the absorbance of the control and A_1 corresponds to that of the sample.

ABTS radical scavenging assay

The antioxidant potential of the extracts was assessed using the $ABTS^{\bullet+}$ decolorization method. Briefly, the ABTS radical cation was produced by mixing ABTS solution with potassium persulfate and allowing the

reaction mixture to stand in the dark at room temperature for 16 h. Before analysis, the resulting $ABTS^{+}\bullet$ solution was diluted with methanol to achieve an absorbance of approximately 0.7–0.8 at 734 nm. Extract samples were prepared at concentrations of 1, 10, 100, and 1000 μg/mL. The assay mixture containing 130 μL of the prepared $ABTS^{+}\bullet$ solution and 20 μL of sample extract was incubated in the dark at room temperature for 6 min, after which absorbance was recorded at 734 nm using a microplate reader. The percentage of radical scavenging activity was determined using the same equation applied in the DPPH assay.

Antibacterial activity

The antibacterial activity of *C. gigantea* leaf extracts was evaluated using the agar well diffusion method against seven bacterial strains, including *Enterococcus faecalis* (ATCC 19433), *Escherichia coli* (ATCC 25922), *Pseudomonas aeruginosa* (ATCC 27853), *Salmonella enterica* serovar Typhimurium (ATCC 14028), *Staphylococcus aureus* (ATCC 25923), *Klebsiella pneumoniae* (KCTC 2690), and *Staphylococcus epidermidis* (ATCC 12228). Briefly, bacterial cultures were grown in Luria–Bertani (LB) broth at 37 °C for 24 h and adjusted to approximately 10^8 CFU/mL. The bacterial suspensions were evenly spread onto LB agar plates using sterile cotton swabs, and wells of 7 mm diameter were aseptically prepared using a sterile cork borer. Extract solutions prepared in dimethyl sulfoxide (DMSO) and sterilized by membrane filtration were introduced into each well. DMSO was employed as the negative control, while ampicillin was used as the positive control. After incubation at 37 °C for 24 h, antibacterial activity was evaluated by determining the diameter of the inhibition zones (mm). All assays were conducted in triplicate.

Isolation and identification

The 70% ethanolic extract (70 g) was suspended in deionized water (100 mL) and sequentially partitioned with solvents of increasing polarity, including *n*-hexane and ethyl acetate (1:1, v/v, three times each), yielding the *n*-hexane (CGHx, 11.7 g), ethyl acetate (CGEA, 26.8 g), and residue (27.5 g) fractions. The *n*-hexane fraction was further separated by normal-phase silica gel column chromatography (CC) using a gradient elution system of *n*-hexane-ethyl acetate (30:1 to 4:1, v/v) to obtain five fractions (CGHx.1–5). Fraction CGHx.3 (3.2 g) was subsequently subjected to normal-phase silica gel column using *n*-hexane-CH_2Cl_2 (10:1, v/v) elution system, affording eight subfractions (CGHx.3.A–G). Subfraction CGHx.3.E (600 mg) was subsequently purified by silica gel column chromatography using an *n*-hexane-CH_2Cl_2 (10:1, v/v) to obtain compound **1** (20.5 mg) and compound **2** (17.4 mg).

β-Sitosterol (**1**): white crystals, ^{1}H-NMR (600 MHz, $CDCl_3$): δ (ppm) 5.35 (1H, *t*; *J* = 2.7 Hz, 2.7 Hz, H-6); 3.52 (1H, *m*, H-3); 1.01 (3H, *s*, H-19); 0.92 (3H, *d*, *J* = 6.6 Hz, H-21); 0.84 (3H, *d*, *J* = 7.2 Hz, H-27); 0.83 (3H, *d*, *J* = 6.6 Hz, H-26); 0.81 (3H, *d*, *J* = 6.6 Hz, H-29), 0.68 (3H, *s*, H-18);

β-Sitostenone (**2**): white crystals, ^{1}H-NMR (600 MHz, $CDCl_3$): δ (ppm) 5.72 (1H, s, H-3); 1.18 (3H, s, H-19); 0.92 (3H, d, *J* =6.0 Hz, H-21); 0.84 (3H, t, *J* = 7.2 Hz, H-29); 0.83 (3H, d, *J* = 6.6 Hz, H-26); 0.81 (3H, d, *J* = 7.2 Hz, H-27), 0.71 (3H, s, H-18).

Molecular docking

To elucidate the interaction mechanism and binding affinity between the isolated phytosterols and antioxidant-related proteins, an in silico molecular docking study was conducted using AutoDock Vina version 1.2[6]. The three-dimensional crystal structures of Superoxide Dismutase (SOD1, PDB ID: 2C9V), Catalase (CAT, PDB ID: 1DGF), and Kelch-like ECH-associated protein 1 (Keap1, PDB ID: 8IXS) were obtained from the RCSB Protein Data Bank. Protein preparation was carried out in BIOVIA Discovery Studio Visualizer 2025, removing water molecules, heteroatoms, and co-crystallized ligands. To optimize the receptor structures, polar hydrogen atoms and partial charges were subsequently assigned. The active site of each enzyme was defined using the "Define and Edit Binding Site" module, targeting key catalytic residues reported in the literature. Ligands (β-sitosterol and β-sitostenone) were subjected to energy minimization using the MMFF94 force field to generate their lowest-energy conformers, which were then converted into PDBQT format. For CAT and Keap1, the docking grids were defined based on the coordinates of the co-crystallized ligands. The reliability of the docking protocol was assessed by re-docking the native ligands into their corresponding binding sites, with RMSD values below 2.0 Å considered acceptable (Supplementary data, Table 5). In the case of SOD1 (PDB ID: 2C9V), no co-crystallized ligand was available to guide binding-site definition; therefore, a blind docking approach was adopted. The grid box was centered on the protein structure and sized to completely encompass the receptor with an additional margin of approximately 10 Å, enabling the

identification of potential binding regions across the entire protein surface. Similar strategies have been widely applied in molecular docking studies when experimental information regarding ligand-binding sites is unavailable[7,8]. The exhaustiveness parameter was set between 8 and 32, and docking poses were ranked according to their predicted binding energies (kcal/mol). The best docking conformations were visualized and analyzed using Discovery Studio, enabling characterization of hydrogen bonding, hydrophobic (alkyl and π–alkyl), and van der Waals interactions between ligands and amino acid residues. Similar docking methodologies have been extensively applied in studies of antioxidant and bioactive natural products, supporting the reliability of this computational approach.

Statistical Analysis

Data analysis was performed using GraphPad Prism version 8.4.3. Results from antioxidant assays are reported as mean ± SD. Comparisons among groups were assessed using one-way or two-way ANOVA with Tukey's multiple comparison post hoc test, and differences were considered statistically significant at $p < 0.05$.

RESULTS AND DISCUSSIONS

Phytochemical screening

Preliminary phytochemical analysis indicated the presence of alkaloids, saponins, reducing sugars, phenolic compounds, flavonoids, coumarins, and terpenoids in *C. gigantea* leaf extracts. As summarized in Table 1, the distribution of these compounds varied according to solvent polarity. Alkaloids and phenolic compounds/tannins were mainly detected in ethanolic extracts, particularly in 70% and 96% ethanol, whereas reducing sugars and saponins were more prominent in the aqueous extract. This pattern suggests that ethanol favored the extraction of moderately polar secondary metabolites, while water was more effective for highly polar constituents.

Antioxidant activity

The antioxidant activity of *C. gigantea* leaf extracts was evaluated using DPPH and ABTS radical scavenging assays. As shown in Table 2, all extracts exhibited radical scavenging activity, with ethanol extracts showing higher activity than the aqueous extract. In the DPPH assay, the 70% ethanol extract showed the strongest activity, reaching 86.31 ± 1.10% inhibition at 1000 μg/mL. This was followed by the 40% ethanol extract (58.31 ± 1.47%), 96% ethanol extract (51.52 ± 1.44%), and aqueous extract (31.89 ± 13.65%). A similar pattern was observed in the ABTS assay at 100 μg/mL, where the 70% ethanol extract again showed the highest scavenging activity (44.54 ± 0.87%), followed by 96% ethanol (39.63 ± 1.86%), 40% ethanol (32.02 ± 0.84%), and aqueous extract (24.48 ± 3.06%).

Data are reported as mean ± SD from three independent measurements. Within the same column, different lowercase letters indicate statistically significant differences as determined by Tukey's multiple comparison test ($p < 0.05$). Most crude extracts did not provide reliable IC_{50} values under the tested concentration range; therefore, antioxidant capacity was expressed as percentage radical scavenging at fixed concentrations. Vitamin C, used as the positive control, exhibited strong concentration-dependent radical scavenging activity in both assays, reaching 96.09 ± 0.20% and 100.08 ± 0.10% inhibition at 16 μg/mL in the DPPH and ABTS assays, respectively.

The concentration–response curves derived from the DPPH and ABTS assays are shown in Figure 1. Plotting the percentage of radical scavenging against the logarithm of extract concentration clearly illustrates the dose-dependent antioxidant responses of the four extracts and supports comparison of their relative antioxidant potencies. Among them, the 70% ethanol extract consistently exhibited the strongest radical scavenging activity.

Antibacterial activity

Antibacterial effects of *C. gigantea* leaf extracts against seven bacterial strains were investigated using the agar well diffusion method. Under the experimental conditions, none of the tested extracts, including aqueous and ethanol extracts (40%, 70%, and 96%), exhibited inhibitory effects against any of the tested microorganisms. No distinct inhibition zones were observed for any of the tested samples. The positive control (ampicillin) showed antibacterial activity against most tested strains. However, *P. aeruginosa* and *K. pneumoniae* did not exhibit sensitivity to ampicillin, indicating intrinsic or acquired resistance under the experimental conditions. No inhibitory effect was observed for the negative control (DMSO). These results suggest that the antibacterial activity of *C. gigantea* may be dependent on plant part, extraction method, or concentration.

Isolation, identification and antioxidant activity of compounds 1 and 2

Among the evaluated extracts, the 70% ethanolic extract of *C. gigantea* leaves demonstrated the highest

Table 1: Phytochemical constituents of *C. gigantea* leaf extracts obtained with different solvents [Source: authors]

Phytochemical	Test/Reagent	Aqueous extract	40% Ethanol extract	70% Ethanol extract	96% Ethanol extract
Alkaloids	Mayer's reagent	–	+	++	++
Saponins	Frothing test	++	+	+	+
Reducing sugars	Fehling's test	+++	++	+	+
Tannins	FeCl3 test	–	+	++	++
Flavonoids	Lead acetate test	++	+	+	+
Coumarins	NaOH test	+	+	+	+
Terpenoids	Liebermann–Burchard test	+	++	++	++

(–) Not detected; (+) weak presence; (++) moderate presence; (+++) strong presence

Table 2: Scavenging effects of aqueous and ethanolic leaf extracts of *C. gigantea* on DPPH and ABTS radicals [Source: authors]

Extract/Sample	DPPH scavenging (%) at 100 μg/mL	DPPH scavenging (%) at 1000 μg/mL	ABTS scavenging (%) at 100 μg/mL	ABTS scavenging (%) at 1000 μg/mL
Water	16.91 ± 8.73^{a}	31.89 ± 13.65^{a}	24.48 ± 3.06^{a}	99.12 ± 0.18^{a}
EtOH 40%	13.87 ± 3.73^{a}	58.31 ± 1.47^{b}	32.02 ± 0.84^{b}	99.03 ± 0.28^{a}
EtOH 70%	20.70 ± 1.97^{a}	86.31 ± 1.10^{c}	44.54 ± 0.87^{c}	99.33 ± 0.13^{a}
EtOH 96%	13.15 ± 1.48^{a}	51.52 ± 1.44^{ab}	39.63 ± 1.86^{c}	97.22 ± 0.08^{a}

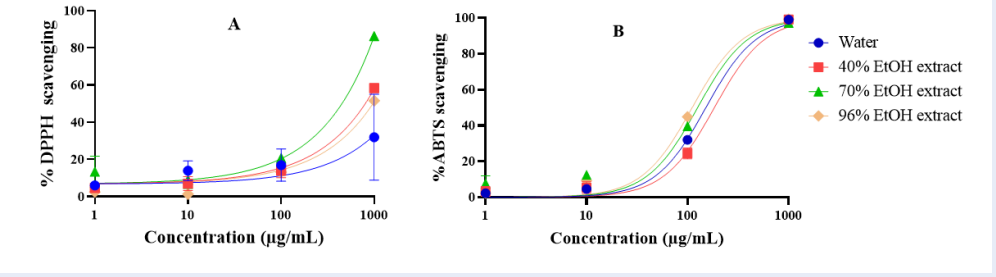

Figure 1: DPPH (A) and ABTS (B) radical scavenging activities of aqueous and ethanolic leaf extracts of *Calotropis gigantea*. [Source: authors]

radical scavenging activity in both DPPH and ABTS assays. Therefore, this extract was selected for further phytochemical investigation. Fractionation of the hexane-soluble fraction resulted in the isolation of two known sterol . Their structures were elucidated through ^{1}H-NMR spectroscopic analysis (Figures 6 and 7) and comparison with previously reported data[9], leading to their identification as β-sitosterol (**1**) and β-sitostenone (**2**) (Figure 2).

The ABTS and DPPH assays also performed with β-sitosterol (**1**) and β-sitostenone (**2**), both sterols exhibited relatively weak radical scavenging activities, although their effects increased in a concentration-dependent manner (Table 3). β-Sitosterol (**1**) displayed relatively weak antioxidant activity throughout the tested concentration range. β-sitosterol (**1**) exhibited weak activity in both assays, reaching only 43.59 $\pm$ 3.38% and 19.87 $\pm$ 6.30% inhibition

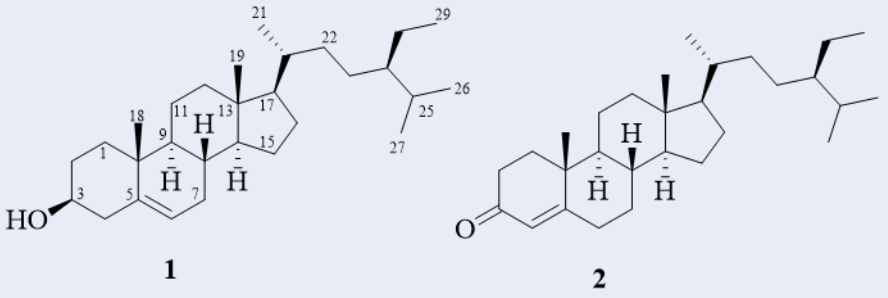

Figure 2: Chemical structure of compounds 1 and 2 from leaf extracts of *C. gigantea*. [Source: ChemDraw 18.0]

Table 3: Scavenging effects of compound 1 and 2 on DPPH and ABTS radicals [Source: authors]

Concentration	Inhibition (%)			
	ABTS		DPPH	
	β-sitosterol (**1**)	β-sitostenone (**2**)	β-sitosterol (**1**)	β-sitostenone (**2**)
125 μg/mL	–	16.07 ± 0.02	–	7.51 ± 0.04
250 μg/mL	–	32.02 ± 0.02	–	10.71 ± 0.05
500 μg/mL	12.33 ± 5.50	59.16 ± 0.03	5.03 ± 9.40	16.82 ± 0.08
1000 μg/mL	27.53 ± 8.03	86.85 ± 0.02	10.34 ± 7.10	23.37 ± 0.12
2000 μg/mL	43.59 ± 3.38	97.58 ± 0.01	19.87 ± 6.30	30.91 ± 0.13

"–": Not detected or inhibition activity was below the measurable limit under the experimental conditions.

against ABTS and DPPH radicals, respectively, at 2000 μg/mL. While β-sitostenone (**2**) displayed comparatively higher activity, particularly in the ABTS assay, with inhibition increasing to 97.58 ± 0.01% at 2000 μg/mL, while DPPH scavenging remained modest (30.91 ± 0.13%).

Molecular docking analysis of compounds 1 and 2

The predicted binding affinities of β-sitosterol (1) and β-sitostenone (2) toward the three antioxidant-related protein targets are summarized in Table 4. Both compounds exhibited favorable interactions with SOD1, CAT, and Keap1, with the strongest binding observed for Keap1. Overall, β-sitostenone showed slightly higher binding affinity than β-sitosterol, particularly against Keap1 (−10.3 kcal/mol versus −9.9 kcal/mol), suggesting a stronger potential for modulating the Keap1/Nrf2 antioxidant pathway.

Compound **1** exhibited moderate to strong binding affinities toward all selected antioxidant-related protein targets, including SOD1, CAT, and Keap1, with binding energies of −7.4, −8.7, and −9.9 kcal/mol, respectively. In the SOD1 complex, the ligand occupied the hydrophobic cavity and was stabilized predominantly through Van der Waals and alkyl interactions involving residues Ile151, Ile113, Cys111, and Leu106. In the CAT complex, compound **1** inserted deeply into the hydrophobic enzyme cavity and formed extensive alkyl, π–alkyl, π–sigma, and Van der Waals interactions with residues including His305 and Phe198, resulting in a relatively strong binding affinity of −8.7 kcal/mol. Among all targets, the strongest interaction was observed with Keap1, where compound **1** achieved a binding energy of −9.9 kcal/mol. The ligand formed a stabilizing hydrogen bond with Val465 together with dense hydrophobic interactions involving Ala366, Ala556, Arg415, and surrounding nonpolar residues. Representative 3D binding poses and 2D interaction diagrams of compound **1** docked with SOD1, CAT, and Keap1 are presented in Figure 3, highlighting the major amino acid residues involved in ligand binding.

Compound **2** demonstrated slightly stronger docking profiles than compound **1**, particularly against Keap1, where the binding energy reached −10.3 kcal/mol. In the SOD1 complex, the ligand adopted a compact hydrophobic conformation stabilized mainly through Van der Waals and alkyl interactions with Cys111,

Table 4: Molecular docking interaction of compound 1 and 2. [Source: authors]

Protein (PDB ID)	Binding energy (kcal/mol)	Interactions	Binding energy (kcal/mol)	Interactions
		β-sitosterol (1)		**β-sitostenone (2)**
SOD1 (2C9V)	−7.4	• Van der Waals: Asp109, Ser107, Arg115, Thr2, Ala4, Lys3 • Alkyl: Ile151, Ile113, Cys111, Leu106	−7.9	• Van der Waals: Asp109, Gly108, Ser107, Arg115, Thr2, Ala152, Lys3, Ile151, Ile113, Leu106 • Alkyl: Cys111, Ile151, Ile113
CAT (1DGF)	−8.7	• Van der Waals: Asn449, Pro304, Phe446, Thr150, Arg203, Ser201, Tyr215, His194 • π-Sigma: His305, Phe198 • Alkyl: Val302, Pro151, Ala445, Val450 • π-Alkyl: Phe198	−9.1	• Van der Waals: Pro304, His305, Asn149, Phe446, Thr150, Arg203, Ser201, Tyr215, His194 • Alkyl: Val302, Pro151, Ala445, Val450 • π-Alkyl: Phe198
Keap1 (8IXS)	−9.9	• Van der Waals: Val418, Gly417, Ile416, Ala510, Gln530, Tyr525, Ser602, Ser555, Ser508, Gly509, Leu557, Gly511, Gly484, Val463, Ile559, Val512, Gly603, Gly462, Val604, Gly364, Gly367, Ala466, Gly605, Leu365 • Conventional Hydrogen Bond: Val465 • Alkyl: Ala366, Ala556, Arg415	−10.3	• Van der Waals: Val465, Val418, Gly417, Ile416, Ala510, Tyr525, Ser555, Ser508, Gly509, Leu557, Gly511, Val463, Ile559, Val512, Gly603, Gly462, Val604, Gly364, Gly367, Ala366, Gly605, Leu365, Gly464, Gly558, Val606 • Alkyl: Ala556, Arg415

Ile151, Ile113, and Leu106. For CAT, compound **2** displayed strong affinity (−9.1 kcal/mol), mainly maintained through hydrophobic and π–alkyl interactions with Phe198. In the Keap1 complex, compound 2 formed an especially stable protein–ligand complex with a binding energy of −10.3 kcal/mol, which was slightly stronger than that observed for compound **1** (−9.9 kcal/mol). The ligand was stabilized through extensive hydrophobic and Van der Waals interactions involving Val418, Gly417, Ala510, Arg415, and adjacent residues. To further illustrate the docking results, representative binding conformations and interaction profiles of compound **2** with SOD1, CAT, and Keap1 are shown in Figure 4.

DISCUSSION

The phytochemical screening results suggest that ethanol favored the extraction of moderately polar secondary metabolites, while water was more effective for highly polar constituents. The present findings are supported by previous reports demonstrating the occurrence of alkaloids, tannins, saponins, flavonoids, phenols, diterpenes, and phytosterols in *C. gigantea* leaves and other plant parts [10,11]. The superior antioxidant potential of the 70% ethanolic extract could be explained by the intermediate polarity of this solvent system, which favors the extraction of antioxidant-associated constituents such as phenolic compounds, flavonoids, tannins, coumarins, and triterpenoids. This interpretation is consistent with the phytochemical screening results, in which phenolics/tannins and triterpenoids were more evident in ethanolic extracts than in the aqueous extract. The present results are consistent with previous studies on *C. gigantea* leaves, in which hydroalcoholic extracts showed strong DPPH radical scavenging activity and contained phenolic compounds, tannins, and

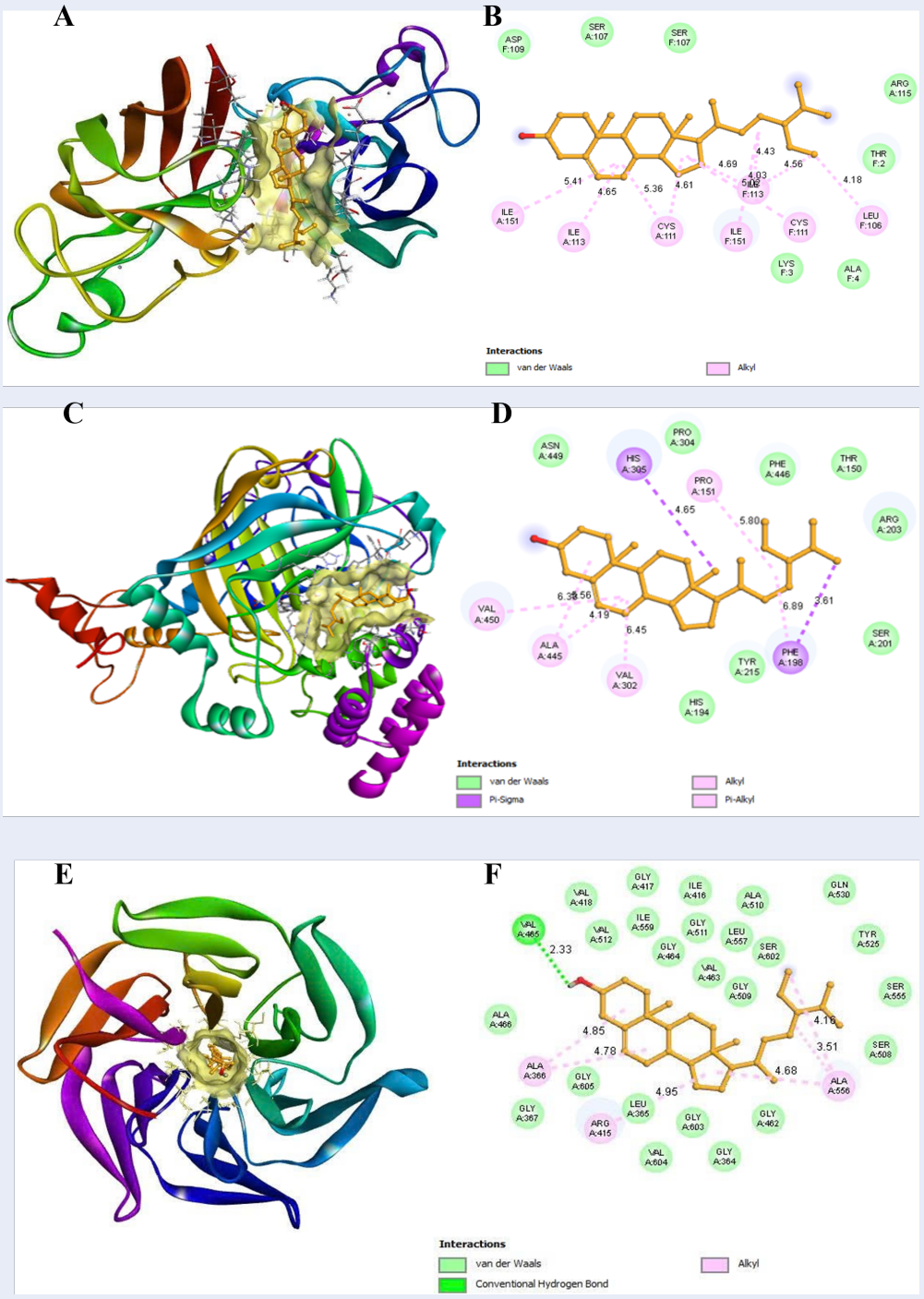

Figure 3: 3D docking poses and 2D interaction diagrams of compound 1 with SOD1 (2C9V) (A, B), CAT (1DGF) (C, D), and Keap1(8IXS) (E, F). [Source: authors + Images were generated using BIOVIA Discovery Studio Visualizer 2025]

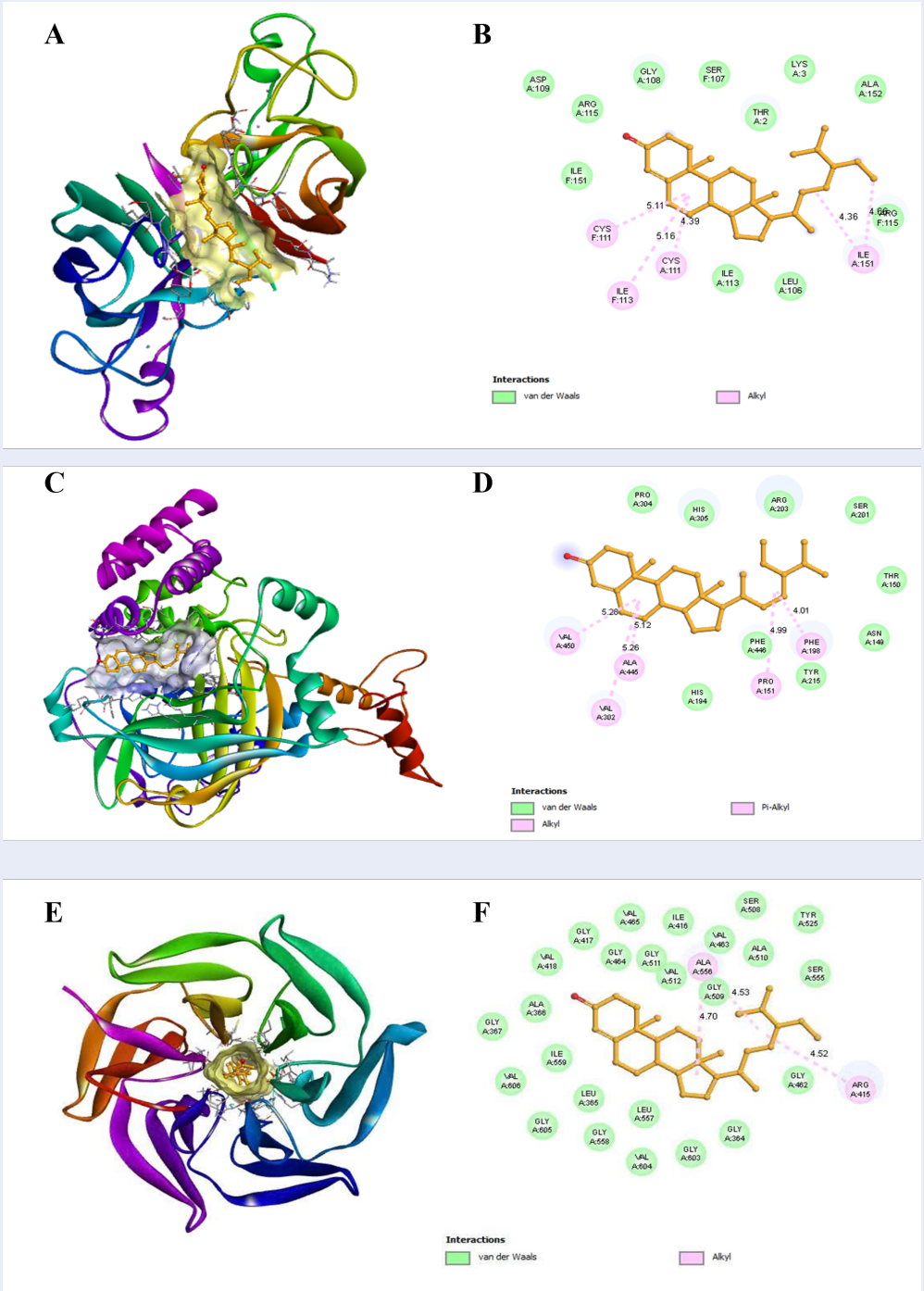

Figure 4: 3D docking poses and 2D interaction diagrams of compound 2 with SOD1 (2C9V) (A, B), CAT (1DGF) (C, D), and Keap1 (8IXS) (E, F). [Source: Authors + Images were generated using BIOVIA Discovery Studio Visualizer 2025]

flavonoids. Other studies also reported antioxidant activity in *C. gigantea* leaves and identified phenolics, flavonoids, and carotenoids as major phytochemical constituents [11,12]. These findings support the important role of polar and semi-polar phytochemicals in contributing to the antioxidant potential of *C. gigantea* leaves. The absence of antibacterial activity in the present study suggests that the antimicrobial potential of C. gigantea may vary depending on factors such as the plant part used, extraction solvent, phytochemical composition, and geographical origin of the collected material. Although previous studies have reported antibacterial properties of *C. gigantea*, variations in environmental conditions and harvesting regions may influence the accumulation of bioactive secondary metabolites and consequently affect the observed biological activity.

β-Sitosterol (**1**) and β-sitostenone (**2**) were isolated from the 70% ethanolic extract, which exhibited the highest antioxidant activity among the tested extracts. However, despite their occurrence in the most active extract, both phytosterols displayed only weak to moderate radical scavenging activities, indicating that they are unlikely to be the principal contributors to the direct DPPH and ABTS scavenging effects of the crude extract. This observation is consistent with previous reports describing phytosterols as relatively poor direct radical scavengers but potential modulators of oxidative stress-related pathways [13–15]. Therefore, the antioxidant contribution of β-sitosterol and β-sitostenone may involve mechanisms beyond direct free-radical quenching. Accumulating evidence suggests that phytosterols can regulate cellular antioxidant defense systems, particularly pathways associated with redox signaling and antioxidant enzymes [13,14,16]. Accordingly, molecular docking analysis was conducted to further investigate their potential interactions with oxidative stress-associated targets, including Keap1, SOD1, and CAT.

The Keap1–Nrf2 signaling pathway represents one of the primary cellular defense systems against oxidative stress. Under physiological conditions, Keap1 binds Nrf2 through its Kelch domain and promotes Nrf2 ubiquitination and proteasomal degradation. Structural studies have identified Arg415, Arg483, Ser508, Tyr525, and Tyr572 as critical residues involved in recognition and stabilization of the ETGE motif of Nrf2 [17–20]. Disruption of these interactions may facilitate Nrf2 nuclear translocation and subsequent activation of antioxidant response element (ARE)-regulated genes, including antioxidant enzymes such as SOD and CAT [21,22]. Among the targets investigated, Keap1 provided the strongest mechanistic support for the antioxidant potential of the isolated phytosterols. Both β-sitosterol and β-sitostenone occupied the Kelch binding pocket and interacted with residues implicated in Nrf2 recognition, particularly Arg415, Ser508, and Tyr525. Since Arg415 and Ser508 contribute to the hydrogen-bonding network that anchors the ETGE motif of Nrf2, while Tyr525 participates in stabilization of the Nrf2-binding cavity [17,18], interactions at these positions may interfere with Keap1–Nrf2 complex formation. Such binding behavior suggests a potential capacity of both compounds to alleviate Keap1-mediated repression of Nrf2 and thereby enhance endogenous antioxidant defenses. Furthermore, β-sitostenone exhibited a slightly stronger binding affinity (-10.3 kcal/mol) than β-sitosterol (-9.9 kcal/mol), indicating that oxidation of the C-3 hydroxyl group to a carbonyl functionality may improve accommodation within the Keap1 binding cavity. Notably, the binding affinities of both phytosterols were comparable to that of the co-crystallized ligand T6I (-9.9 kcal/mol), supporting the plausibility of the predicted binding mode.

In addition to modulation of antioxidant signaling, maintenance of enzymatic ROS detoxification is equally important for cellular redox balance. SOD1 catalyzes the conversion of superoxide radicals into hydrogen peroxide and molecular oxygen, representing the first enzymatic barrier against ROS accumulation. Although the catalytic activity of SOD1 is governed by a conserved Cu/Zn center coordinated by His46, His48, His63, His120, His71, His80, and Asp83 [23,24], neither compound directly interacted with these catalytic residues. Instead, both ligands were localized near residues spanning Leu106–Arg115, a region associated with the electrostatic loop that contributes to structural stability and substrate guidance toward the catalytic center. Therefore, while direct modulation of catalytic metal coordination appears unlikely, interactions within this region may contribute to preservation of the conformational environment required for efficient superoxide dismutation. Consistent with this interpretation, β-sitostenone displayed a slightly stronger affinity (-7.9 kcal/mol) than β-sitosterol (-7.4 kcal/mol), suggesting a modestly enhanced interaction with the structural surface surrounding the electrostatic loop. The hydrogen peroxide generated by SOD1 is subsequently detoxified by CAT, which converts hydrogen peroxide into water and molecular oxygen, thereby preventing oxidative damage caused by excessive peroxide accumulation. The catalytic activity of CAT relies on a buried heme center accessed through a

substrate channel lined by several residues that regulate substrate entry and orientation [25]. Interestingly, both compounds exhibited favorable binding within this substrate-access region, interacting with residues including His194, Phe198, Ser201, Arg203, Tyr215, and His305. Previous structural studies have suggested that residues lining the access channel play important roles in directing hydrogen peroxide toward the catalytic heme and maintaining catalytic efficiency, with Arg203 being particularly relevant for substrate orientation and stabilization [25]. Therefore, the observed interactions may influence the microenvironment surrounding the catalytic pathway rather than the catalytic center itself. Similar to the Keap1 and SOD1 docking results, β-sitostenone displayed slightly stronger binding (−9.1 kcal/mol) than β-sitosterol (−8.7 kcal/mol). Furthermore, the docking scores of both phytosterols were comparable to that of the co-crystallized ligand NADPH (−8.7 kcal/mol), supporting the reliability of the predicted binding poses. Taken together, the docking results suggest that the antioxidant potential of β-sitosterol and β-sitostenone may involve complementary mechanisms acting at different levels of the cellular antioxidant network.

Collectively, the docking analysis indicates that β-sitosterol (**1**) and β-sitostenone (**2**) may influence cellular redox homeostasis through interactions with multiple components of the antioxidant defense system. The preferential association of both compounds with functionally important residues within the Keap1 binding pocket suggests a potential involvement of the Keap1–Nrf2 signaling pathway, whereas the interactions observed with SOD1 and CAT may contribute to stabilization of protein structure or maintenance of enzyme activity.

CONCLUSION

In summary, the present study offers a comprehensive assessment of the phytochemical composition and biological activities of *C. gigantea* leaf extracts. The findings indicate that the leaves constitute a rich source of bioactive secondary metabolites, particularly phenolic compounds and flavonoids, which contribute to a significant concentration-dependent antioxidant capacity. The isolation of β-sitosterol and β-sitostenone, coupled with *in silico* molecular docking, highlights their potential role in modulating the Keap1/Nrf2 signaling pathway, offering a mechanistic basis for the plant's antioxidant properties at the molecular level. Although the extracts showed no direct antibacterial effects under the tested conditions, their potent radical-scavenging ability underscores their value in managing oxidative stress-related disorders. These results support the potential development of *C. gigantea* leaf-based therapeutic agents and emphasize the need for future *in vivo* studies to validate the involvement of Nrf2 activation in order to further clarify its pharmacological potential.

LIST OF ABBREVIATIONS

DPPH: 2,2-diphenyl-1-picrylhydrazyl
ABTS: 2,2'-azino-bis(3-ethylbenzothiazoline-6- sulfonic acid)
SOD1: Superoxide Dismutase 1
CAT: Catalase
Keap1: Kelch-like ECH-associated protein 1
Nrf2: Nuclear factor erythroid 2-related factor 2
ROS: Reactive Oxygen Species
LB: Luria–Bertani
DMSO: Dimethyl Sulfoxide
ARE: Antioxidant Response Element

AUTHOR CONTRIBUTIONS

L. V. H. Tran: conceptualization, investigation, methodology, writing – original draft preparation, writing – review and editing; **T. D. Huynh:** investigation, data analysis; **T. H. H. Nguyen:** investigation, writing – review and editing; **T. M. D. Chung:** investigation, data analysis.

COMPETING INTERESTS

The authors declare that they have no known financial interests or personal relationships that could have appeared to influence the work reported in this paper.

DECLARATION OF GENERATIVE AI USE

The authors confirm that generative or AI-assisted technologies were used solely for grammatical editing and language refinement, and not for generating data or substantive content in this manuscript.

ACKNOWLEDGEMENTS

This research was funded by the University of Medicine and Pharmacy at Ho Chi Minh city under contract 467/2025/HĐ-ĐHYD, dated 30/9/2025.

SUPPLEMENTARY DATA

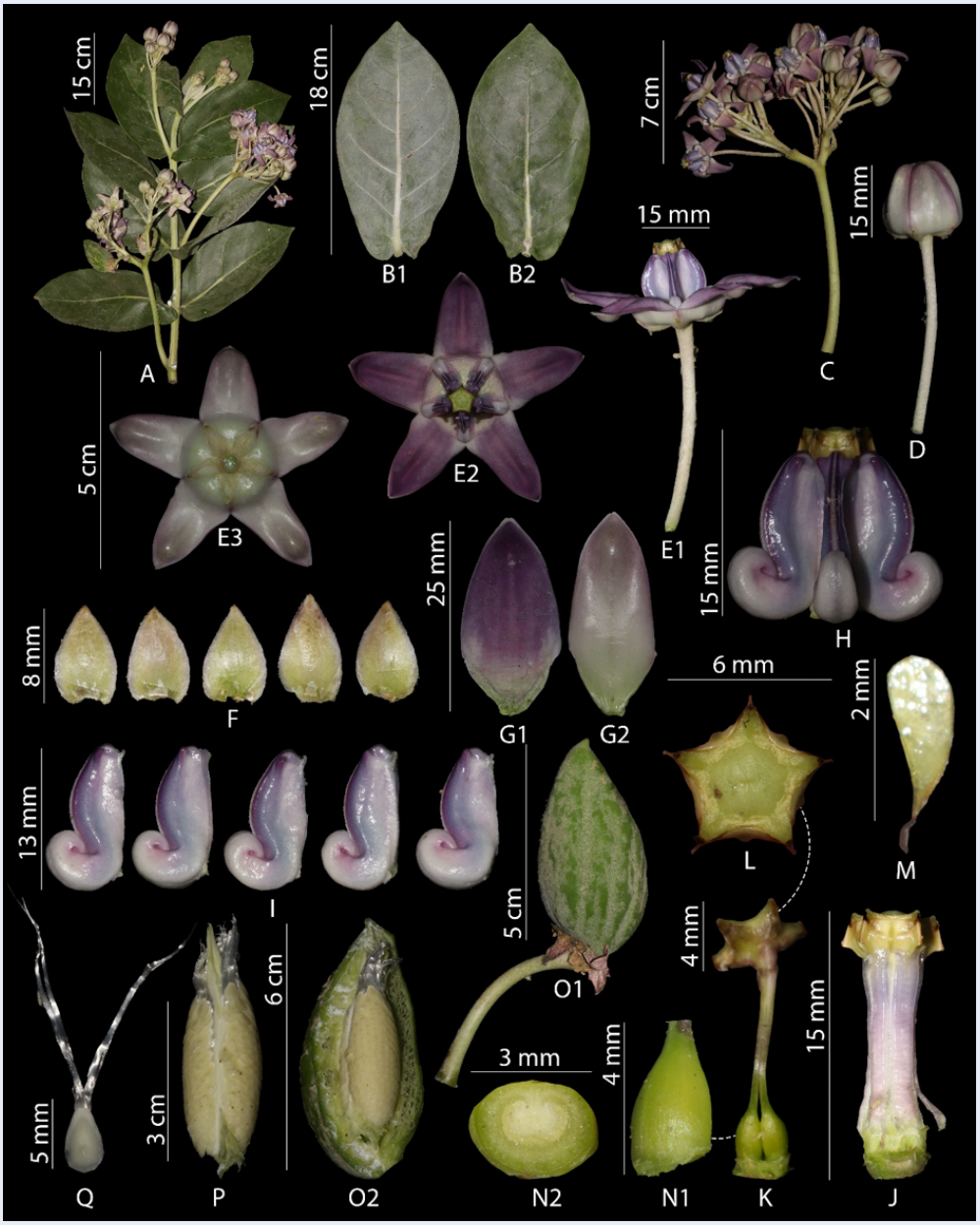

Figure 5: Morphological characteristics of *Calotropis gigantea*, flowering branch (A); adaxial and abaxial leaf surfaces(B1–B2); inflorescence (C); flower bud (D); flower (E1–E3); corona lobes (F) ; corolla lobes(G1–G2); gynostegium with corona (H); isolated corona lobes (I); gynostegium (J-K); stigma head (L); pollinium (M); ovary (N1); transverse section of ovary (N2); follicle (O1); longitudinal section of follicle (O2); seeds (P–Q). [Source: authors]

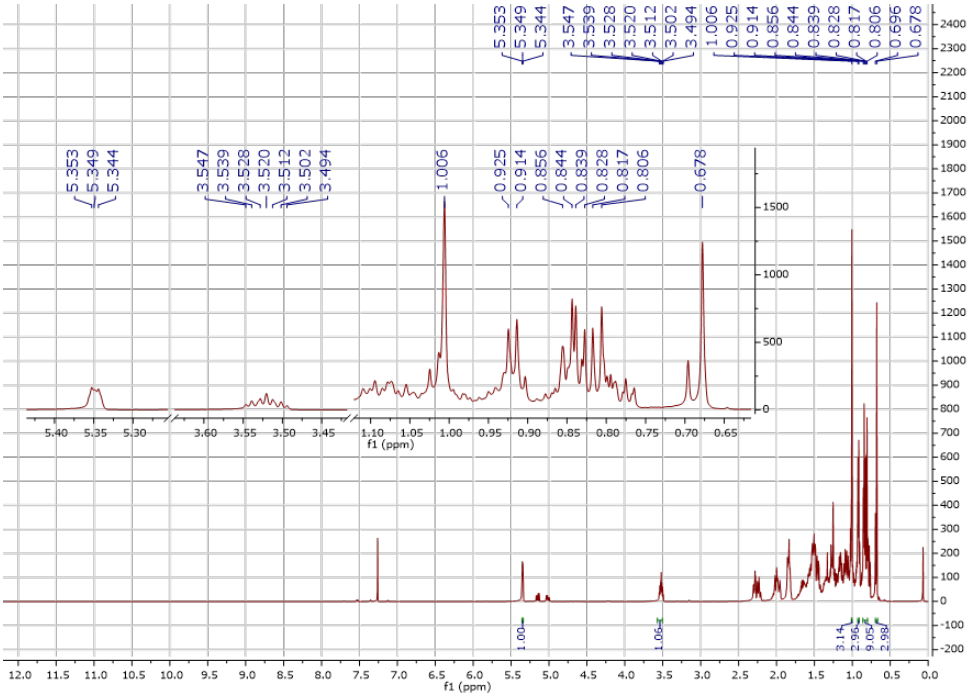

Figure 6: ^{1}H-NMR spectrum of β-sitosterol (1) measuredin $CDCl_3$ at 600MHz. [Source: authors]

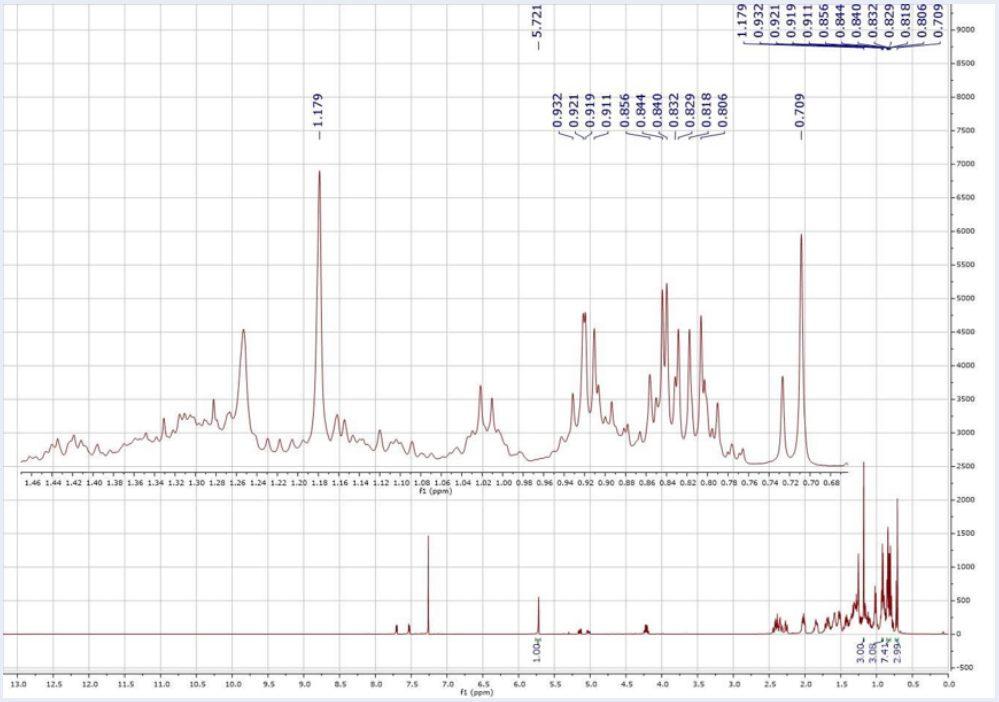

Figure 7: ^{1}H-NMR spectrum of β-sitostenone (2) measured in $CDCl_3$ at 600 MHz. [Source: authors]

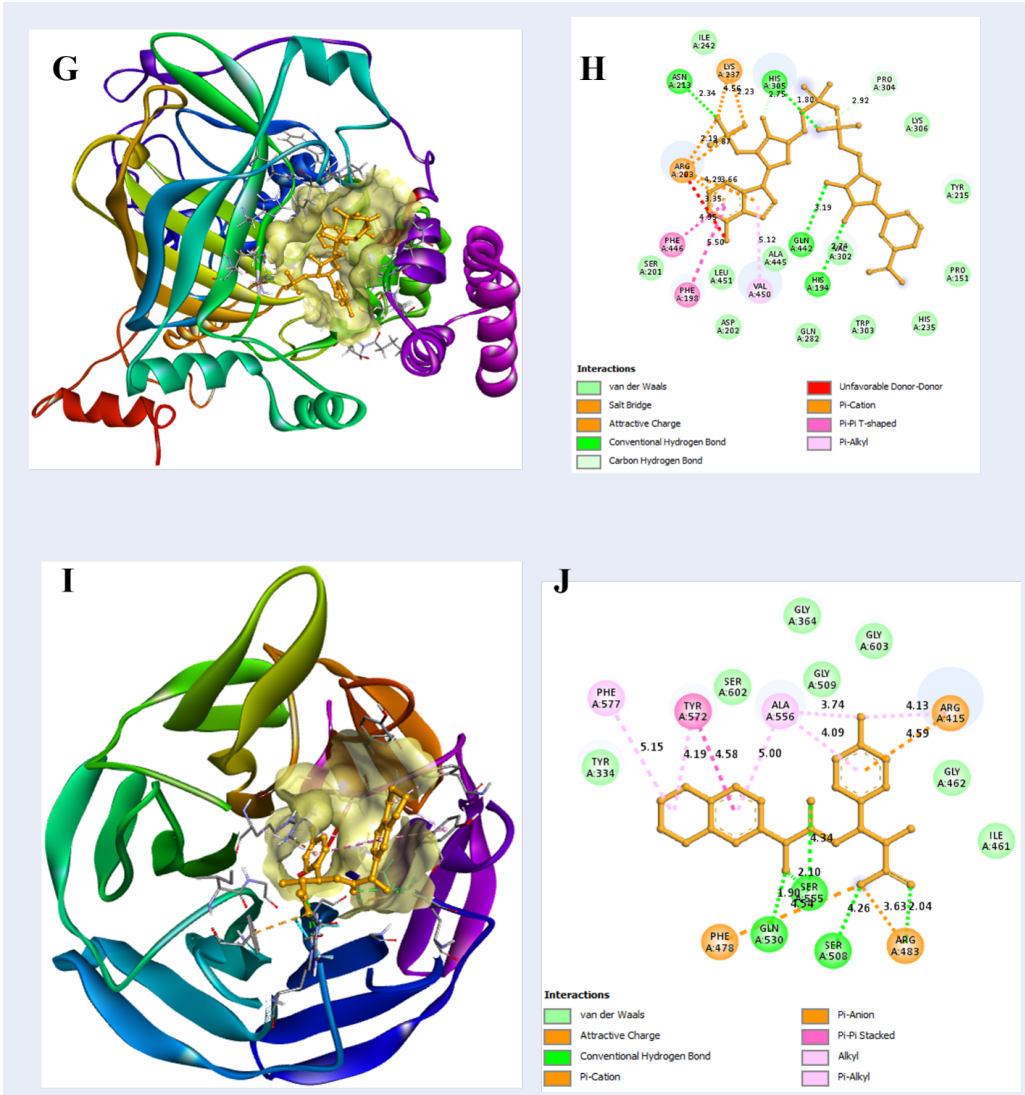

Figure 8: 3D docking poses and 2D interaction diagrams of theco-crystallized ligands with CAT (1DGF) (G, H) and Keap1 (8IXS) (I, J). [Source: Authors + Images were generated using BIOVIA Discovery Studio Visualizer 2025]

Table 5: Docking grid settings and re-docking validation results for the investigated protein targets. [Source: authors]

Protein	PDB ID	Box center coordinates (X, Y, Z)	Box dimensions (Å)	RMSD of the co-crystallized ligand
Keap1	8IXS	14.287; 64.88; 28.648	30 x 24 x 26	0.3101
SOD1	2C9V	20.031; -0.023; 13.897	35 x 43 x 36	-
CAT	1DGF	27.374; 75.422; 69.618	20 x 20 x 20	0.9492

Annotation: RMSD values are reported for proteins containing co-crystallized ligands (KEAP1 and CAT). SOD1 was subjected to blind docking due to the absence of a suitable co-crystallized ligand.

Table 6: Molecular docking interaction ofco-crystallized ligands. [Source: authors]

Protein (PDB ID)	Co-crystallized ligands	Binding energy (kcal/mol)	Interactions
CAT (1DGF)	NADPH (dihydronicotinamide-adenine-dinucleotide phosphate)	−8.7	• Van der Waals: Ile242, Ser201, Asp202, Leu451, Ala445, Gln282, Trp303, His194, His235, Pro151, Tyr215, Lys306. • π-Cation: Arg203 • Carbon Hydrogen Bond: Pro304 • π-π T-shaped: Phe446, Phe198 • Unfavorable Donor-Donor: Arg203 • Salt Bridge: Lys237, Arg203 • Attractive Charge: Lys237, Arg203 • π-Alkyl: Val450 • Conventional Hydrogen Bond: Asn213, His305, Val302, Gln442
KEAP1 (8IXS)	T6I ((2R,3S)-3-[[(2S)-2-fluoranyl-2-(5,6,7,8-tetrahydronaphthalen-2-yl)ethanoyl]amino]-2-methyl-3-(4-methylphenyl)propanoic acid)	−9.9	• Van der Waals: Tyr334, Ser602, Gly364, Gly509, Gly603, Gly462, Ile461. • Conventional Hydrogen Bond: Gln530, Ser555, Ser508, Arg483. • Alkyl: Ala556, Arg415 • π-Alkyl: Phe577, Ala556, Arg415, Tyr572 • π-π Stacked: Tyr572 • π-Cation: Arg415 • π-Anion: Phe478 • Attractive Charge: Arg483

REFERENCES

1. Jomova K, Alomar SY, Alwasel SH, Nepovimova E, Kuca K, Valko M. Several lines of antioxidant defense against oxidative stress: antioxidant enzymes, nanomaterials with multiple enzyme-mimicking activities, and low-molecular-weight antioxidants. Archives of Toxicology. 2024;98(5):1323–67. Available from: https://doi.org/10.1007/s00204-024-03696-4.
2. Kansanen E, Kuosmanen SM, Leinonen H, Levonen AL. The Keap1-Nrf2 pathway: mechanisms of activation and dysregulation in cancer. Redox Biology. 2013;1(1):45–9. Available from: https://doi.org/10.1016/j.redox.2012.10.001.
3. Alafnan A, Sridharagatta S, Saleem H, Khurshid U, Alamri A, Ansari SY, et al. Evaluation of the Phytochemical, Antioxidant, Enzyme Inhibition, and Wound Healing Potential of Calotropis gigantea (L.) Dryand: A Source of a Bioactive Medicinal Product. Frontiers in Pharmacology. 2021;12. Available from: https://doi.org/10.3389/fphar.2021.701369.
4. Kori P, Alawa P. Antimicrobial activity and phytochemical analysis of Calotropis gigantea root, latex extracts. IOSR Journal of Pharmacy (IOSRPHR). 2014;1(2):7–11. Available from: https://doi.org/10.9790/3013-04060207011.
5. Harborne JB. Phytochemical methods: a guide to modern techniques of plant analysis. London: Chapman Hall; 1998.
6. Trott O, Olson AJ. AutoDock Vina: improving the speed and accuracy of docking with a new scoring function, efficient optimization, and multithreading. Journal of Computational Chemistry. 2010;31(2):455–61. Available from: https://doi.org/10.1002/jcc.21334.
7. Meng XY, Zhang HX, Mezei M, Cui M. Molecular docking: a powerful approach for structure-based drug discovery. Current Computer-Aided Drug Design. 2011;7(2):146–57. Available from: https://doi.org/10.2174/157340911795677602.
8. Ferreira LG, Santos RND, Oliva G, Andricopulo AD. Molecular docking and structure-based drug design strategies. Molecules (Basel, Switzerland). 2015;20(7):13384–421. Available from: https://doi.org/10.3390/molecules200713384.
9. Nay K, Tun K, Aminah S, Kristanti A, Zahrah H, Takaya Y. Beta-Sistosterol and beta-sitostenone from Eucalyptus deglupta. Journal of the Indian Chemical Society. 2020;97:779–82.
10. Jamal A, Arif A, Kiran S, Shahid MN, Hossain MB. Phytochemical Investigations and Pharmacological Potential of Organic Extracts of Calotropis gigantea L. Leaves. Scientifica. 2025;2025(1). Available from: https://doi.org/10.1155/sci5/1669969.
11. Rehman N, Haq F. Phytochemical Analysis and Antioxidant Potential of Calotropis procera and Calotropis gigantea. 2023 Aug 7; 2023. Available from: https://doi.org/10.17311/ajbs.2023.254.263.
12. Singh N, Jain NK, Kannojia P, Garud N, Pathak A, Mehta S. In vitro antioxidant activity of Calotropis gigantea hydroalcohlic leaves extract. 2.3; 2010.
13. Arivarasu L. In-vitro antioxidant potential of beta-sitosterol: a preface. Cureus. 2023;15(9). Available from: https://doi.org/10.7759/cureus.45617.
14. Cheng Q, Zhang Y, Lin Q, Tian Y, Bao Y. Study on the antioxidant activity of β-sitosterol and stigmasterol from Sacha Inchi oil and Prinsepia oil added to walnut oil. Food Science and Technology (Campinas). 2022;42. Available from: https://doi.org/10.1590/fst.69522.

15. Ruksilp T. Fatty Acids and an Ester from the Leaves of Millettia utilis Dunn; 2020. Available from: https://doi.org/10.14456/nujst.2020.26.
16. Shen M, Yuan L, Zhang J, Wang X, Zhang M, Li H, et al. Phytosterols: physiological functions and potential application. Foods. 2024;13(11):1754. Available from: https://doi.org/10.3390/foods13111754.
17. Lo SC, Li X, Henzl MT, Beamer LJ, Hannink M. Structure of the Keap1:Nrf2 interface provides mechanistic insight into Nrf2 signaling. The EMBO Journal. 2006;25(15):3605–17. Available from: https://doi.org/10.1038/sj.emboj.7601243.
18. Canning P, Sorrell FJ, Bullock AN. Structural basis of Keap1 interactions with Nrf2. Free Radical Biology Medicine. 2015;88:101–7. Available from: https://doi.org/10.1016/j.freeradbiomed.2015.05.034.
19. Huenchuguala S, Segura-Aguilar J. Natural compounds that activate the KEAP1/Nrf2 signaling pathway as potential new drugs in the treatment of idiopathic Parkinson's disease. Antioxidants. 2024;13(9):1125. Available from: https://doi.org/10.3390/antiox13091125.
20. Zou L, Yu X, Cai K, Xu B, Chen C, Xiao G. Identification of antioxidant peptides targeting Keap1-Nrf2-ARE pathway from in vitro digestion of pork sausage with partial substitution of NaCl by KCl. Food Research International. 2023;174(Pt 1). Available from: https://doi.org/10.1016/j.foodres.2023.113585.
21. Ma Q. Role of nrf2 in oxidative stress and toxicity. Annual Review of Pharmacology and Toxicology. 2013;53(1):401–26. Available from: https://doi.org/10.1146/annurev-pharmtox-011112-140320.
22. Yamamoto M, Kensler TW, Motohashi H. The KEAP1-NRF2 system: a thiol-based sensor-effector apparatus for maintaining redox homeostasis. Physiological Reviews. 2018;98(3):1169–203. Available from: https://doi.org/10.1152/physrev.00023.2017.
23. Tainer JA, Getzoff ED, Beem KM, Richardson JS, Richardson DC. Determination and analysis of the 2 A-structure of copper, zinc superoxide dismutase. Journal of Molecular Biology. 1982;160(2):181–217. Available from: https://doi.org/10.1016/0022-2836(82)90174-7.
24. Valentine JS, Doucette PA, Potter SZ. Copper-zinc superoxide dismutase and amyotrophic lateral sclerosis. Annual Review of Biochemistry. 2005;74(1):563–93. Available from: https://doi.org/10.1146/annurev.biochem.72.121801.161647.
25. Chelikani P, Fita I, Loewen PC. Diversity of structures and properties among catalases. Cellular and Molecular Life Sciences : CMLS. 2004;61(2):192–208. Available from: https://doi.org/10.1007/s00018-003-3206-5.

VNUHCM Journal of Health Sciences 2026, 7(2):1156-1172

Open Access Full Text Article

Bài nghiên cứu

Nghiên cứu thành phần hóa học, hoạt tính chống oxy hóa và phân tích docking phân tử của các sterol từ lá cây Bồng bồng (*Calotropis gigantea*)

Trần Lê Việt Hà*, Huỳnh Thanh Duy, Nguyễn Thị Hồng Hiếu, Chung Thị Mỹ Duyên

Use your smartphone to scan this QR code and download this article

TÓM TẮT

Mở đầu: *Calotropis gigantea* (L.) R. Br. ex Schult. từ lâu đã được sử dụng trong y học cổ truyền để hỗ trợ điều trị các bệnh lý viêm và các tình trạng liên quan đến stress oxy hóa. Các nghiên cứu trước đây cho thấy loài này chứa nhiều hợp chất chuyển hóa thứ cấp có hoạt tính sinh học tiềm năng; tuy nhiên, thành phần hóa thực vật của các cao chiết lá được điều chế bằng các dung môi có độ phân cực khác nhau, cũng như cơ chế chống oxy hóa tiềm năng của các thành phần chính, vẫn chưa được làm sáng tỏ đầy đủ.

Mục tiêu: Nghiên cứu nhằm khảo sát thành phần hóa thực vật, hoạt tính chống oxy hóa và kháng khuẩn của các cao chiết nước và ethanol từ lá *C. gigantea*; phân lập các hợp chất có hoạt tính sinh học chính từ cao chiết có hoạt tính mạnh nhất; đồng thời khảo sát cơ chế chống oxy hóa tiềm năng của các hợp chất này thông qua phân tích docking phân tử.

Phương pháp: Lá *C. gigantea* được chiết bằng nước và ethanol ở các nồng độ 40%, 70% và 96%. Thành phần hóa thực vật sơ bộ được khảo sát bằng các phản ứng định tính tiêu chuẩn. Hoạt tính chống oxy hóa được đánh giá bằng các phép thử bắt giữ gốc tự do DPPH và ABTS, trong khi hoạt tính kháng khuẩn được khảo sát trên bảy chủng vi khuẩn bằng phương pháp khuếch tán trên thạch. Cao chiết có hoạt tính chống oxy hóa mạnh nhất được phân đoạn bằng phương pháp sắc ký, và các hợp chất phân lập được xác định bằng phổ cộng hưởng từ hạt nhân proton (^{1}H-NMR). Phân tích docking phân tử được thực hiện nhằm đánh giá tương tác của các hợp chất phân lập với các đích liên quan đến chống oxy hóa, bao gồm superoxide dismutase 1 (SOD1), catalase (CAT) và Kelch-like ECH-associated protein 1 (Keap1).

Kết quả: Khảo sát hóa thực vật cho thấy sự hiện diện của alkaloid, hợp chất phenolic, flavonoid, coumarin, terpenoid, đường khử và saponin; trong đó các cao chiết ethanol chứa hàm lượng phenolic và terpenoid cao hơn so với cao chiết nước. Trong số các mẫu khảo sát, cao chiết ethanol 70% thể hiện hoạt tính chống oxy hóa mạnh nhất, với khả năng bắt giữ gốc DPPH đạt 86,31 ± 1,10% ở nồng độ 1000 μg/mL và bắt giữ gốc ABTS đạt 44,54 ± 0,87% ở nồng độ 100 μg/mL. Không ghi nhận hoạt tính kháng khuẩn của bất kỳ cao chiết nào trong điều kiện thí nghiệm. Nghiên cứu hóa thực vật trên cao chiết có hoạt tính mạnh nhất đã phân lập được β-sitosterol (**1**) và β-sitostenone (**2**). Kết quả docking phân tử cho thấy cả hai sterol đều có khả năng liên kết thuận lợi với SOD1, CAT và đặc biệt là Keap1; trong đó β-sitostenone thể hiện ái lực liên kết dự đoán mạnh nhất với Keap1 (−10,3 kcal/mol).

Kết luận: Kết quả cho thấy ethanol 70% là dung môi phù hợp nhất để chiết các hợp chất hóa thực vật liên quan đến hoạt tính chống oxy hóa từ lá *C. gigantea*. Việc phân lập β-sitosterol và β-sitostenone, cùng với khả năng tương tác thuận lợi của hai hợp chất này với các đích liên quan đến chống oxy hóa, đặc biệt là Keap1, gợi ý rằng các sterol này có thể góp phần vào hoạt tính chống oxy hóa của *C. gigantea* thông qua điều hòa con đường tín hiệu Keap1/Nrf2. Những kết quả này cung cấp cơ sở khoa học cho các nghiên cứu tiếp theo về cơ chế tác dụng và thử nghiệm *in vivo*, hướng đến phát triển các tác nhân chống oxy hóa có nguồn gốc từ *C. gigantea*.

Từ khoá: *Calotropis gigantea*, sterol, hoạt tính chống oxy hóa, docking phân tử

Khoa Y học cổ truyền, Đại học Y Dược TP.HCM

Liên hệ

Trần Lê Việt Hà, Khoa Y học cổ truyền, Đại học Y Dược TP.HCM

Email: tlvha@ump.edu.vn

Lịch sử

- Ngày nhận: 15-05-2026
- Ngày sửa đổi: 04-07-2026
- Ngày chấp nhận: 20-07-2026
- Ngày đăng: 14-09-2026

DOI : https://doi.org/10.32508/vnuhcmj-hs.v7i2.788

Check for updates

Trích dẫn bài báo này: Hà T L V, Duy H T, Hiếu N T H, Duyên C T M. **Nghiên cứu thành phần hóa học, hoạt tính chống oxy hóa và phân tích docking phân tử của các sterol từ lá cây Bồng bồng (*Calotropis gigantea*)**. *VNUHCM J. Health Sci.* 2026; 7(2):1156-1172.